JOURNAL OF MATERIALS SCIENCE 25 (1990) 3314–3320

Mössbauer studies of a-$Fe_{74}Co_{10-x}Cr_xB_{16}$ alloys

T. G. NARENDRABABU, R. JAGANNATHAN
School of Chemistry, University of Hyderabad, Hyderabad 500 134, India
V. N. MURTHY, D. AKHTAR, P. SUBRAHMANIAM
Defence Metallurgical Research Laboratory, Hyderabad 500 258, India

Fe^{57} Mössbauer spectroscopy has been employed to study hyperfine interactions in melt-spun a-$Fe_{74}Co_{10-x}Cr_xB_{16}$ (x = 0, 2.5, 5, 7.5 and 10) ribbons. The Curie temperature and the effective hyperfine fields observed for the spectra at 80 K show a systematic fall with increasing chromium content. Increasing chromium content also brings about a change in the orientation of the magnetization axis in that it comes closer to the direction of γ-ray propagation. The temperature dependence of hyperfine fields in a-$Fe_{74}Co_5Cr_5B_{16}$ alloy is accounted for using the existing theoretical models. The field distribution curves show a temperature dependence, while the e.f.g. distribution evaluated from the paramagnetic doublet spectra above T_c are temperature independent. The spin-wave coefficients B ($B_{3/2}$) and C ($C_{5/2}$) and the critical exponent, β, were determined and their significances explained.

1. Introduction

One of the important aspects of current interest in the investigations of iron-rich ferromagnetic metallic glasses is the variation in their physical properties, in particular, thermal and magnetic properties due to composition [1–3]. In such studies investigations on amorphous alloys containing small percentages of vanadium, chromium, manganese, cobalt and molybdenum are invaluable as these elements strongly influence the magnetic and/or thermal properties [4–10]. In this context, we undertook the preparation and characterization of amorphous $Fe_{74}Co_{10-x}Cr_xB_{16}$ (x = 0, 2.5, 5, 7.5 and 10) alloys, the composition being chosen on the basis that cobalt and chromium will have desirable influences on the magnetic and thermal properties, respectively. We have reported earlier the details of preparation and preliminary studies by Mössbauer spectroscopy, X-ray diffraction and differential scanning calorimetry [11–14]. In this work, we report detailed Mössbauer studies of hyperfine interactions on these alloys, especially bringing about those features which distinguish amorphous ferromagnetic alloys from crystalline systems.

2. Experimental procedures

The a-$Fe_{74}Co_{10-x}Cr_xB_{16}$ (x = 0, 2.5, 5, 7.5 and 10) alloys were prepared by melt-spinning. Details of preparation of these alloys have been given elsewhere [11, 13]. The ribbons were around 30 to 40 μm thick and 2 to 3 mm wide. The Mössbauer measurements were made using an Elscint Mössbauer spectrometer. Details of measurements and of the methods of analysing the data are given elsewhere [15–17].

3. Results

3.1. Mössbauer studies as a function of chromium composition

The Mössbauer spectra of a-$Fe_{74}Co_{10-x}Cr_xB_{16}$ (x = 0, 2.5, 5, 7.5 and 10) alloys recorded at 80 K are reproduced in Fig. 1a. These spectra are characterized by asymmetric six-finger patterns with large line widths. In these cases, the relative intensities of the second and fifth lines are more intense than those of the first and the sixth lines [17–21]. The intensity of the second and fifth lines increases in amplitude as a function of chemical composition, as shown by the low-temperature Mössbauer measurements. For a fixed absorber, the average angle between the plane of the ribbon and the magnetization axis, Θ, may be written as [22],

$$\Theta = 90° - \arcsin\left[\frac{\frac{3}{2}(A_{2,5}/A_{1,6})}{1 + \frac{3}{4}(A_{2,5}/A_{1,6})}\right]^{1/2} \quad (1)$$

where $A_{2,5}$ and $A_{1,6}$ correspond to the average areas of the second and fifth and the first and sixth lines, respectively. This relationship is valid for a thin absorber placed perpendicular to the propagation of γ-rays. In the present cases for the spectra at 80 K, the $A_{2,5}/A_{1,6}$ values range from 0.4 to 1.2, showing that the magnetization axis tends to come closer to the direction of γ-rays from Θ = 44° 7′ for x = 0 to Θ = 18° for x = 10 samples, respectively. Similar changes in the Θ values were observed on heating a sample of given composition, as discussed later.

The Curie temperatures (T_c) for these a-alloys were determined by the thermal-scan method [15, 17, 23]. For x = 0 composition, the Curie temperature could not be determined by this method as crystallization precedes the Curie point, confirming our earlier observation on a commercial sample of the same composition [16]. A plot of Curie temperature against chromium content is shown in Fig. 2. The Curie temperatures range from 675 ± 5 K for x = 2.5 to 388 ± 5 for x = 10 samples, indicating a systematic fall in T_c with increasing chromium content.

0022–2461/90 $03.00 + .12

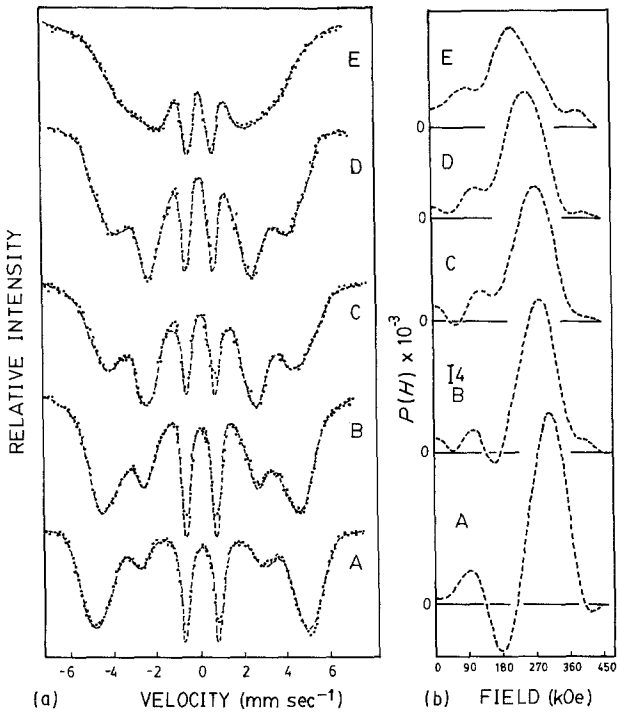

Figure 1 (a) Mössbauer spectra of a-$Fe_{74}Co_{10-x}Cr_xB_{16}$ alloys at 80 K. The dashed line represents theoretical spectra according to Window [24]. (b) Field distribution curves of a-$Fe_{74}Co_{10-x}Cr_xB_{16}$ at 80 K according to Window [24] x = A, 0; B, 2.5; C, 5; D, 7.5; E, 10.

The asymmetry in line widths and line intensities can conveniently be analysed by deconvolution of the experimental spectra in terms of the component spectra, which arise due to the random distribution of atoms in these solids [24–27]. The analysis was carried out by the procedure of Window [24], after optimization of input parameters. This procedure gives rise to symmetric broad theoretical spectra. The small deviations of the theoretical fit from the experimental data are caused by the orientation of the magnetization axis discussed earlier, and the correlation between isomer shift and hyperfine field, which is not taken into account in this procedure. The field distribution curves, $P(H)$, thus obtained for the above spectra, are reproduced in Fig. 1b. All of them exhibit a major peak at higher fields and a minor peak around 90 to 100 kOe. The minor peak arises due to an artefact effect. The important feature is the asymmetry in the major peak which becomes pronounced with increasing chromium content. The $P(H)$ curves are characterized by the most probable field, H_p, the mean field,

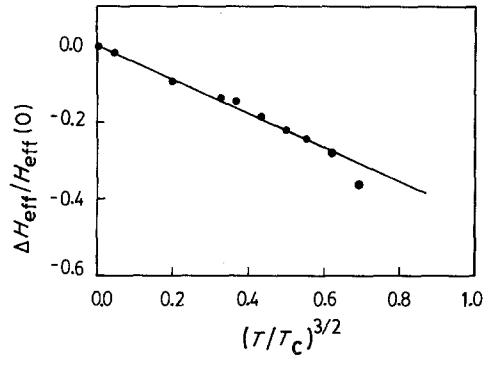

Figure 2 Plot of Curie temperature against chromium concentration for a-$Fe_{74}Co_{10-x}Cr_xB_{16}$ alloys.

TABLE I The most probable field (H_p), mean field (H_{mean}) and full width at half maximum (ΔH) for a-$Fe_{74}Co_{10-x}Cr_xB_{16}$ alloys at 80 K according to Window [24].

Alloy composition	H_p (±3 kOe)	H_{mean} (±3 kOe)	ΔH (±3 kOe)
x = 0	310.5	289.6	103.5
x = 2.5	288.0	264.8	112.5
x = 5	279.0	246.9	119.3
x = 7.5	252.0	228.4	130.5
x = 10	216.0	204.7	151.9

H_{mean}, and the full width at half maximum, ΔH. These parameters are listed as a function of chemical composition in Table I. The theoretical spectra thus simulated when superimposed on the experimental spectra show good agreement. The ΔH value in the above cases is found to increase from 103 kOe for x = 0 samples to 151 kOe for x = 10 samples at 80 K. The H_p and H_{mean} values show a systematic fall, from 310 and 289 kOe for chromium-free samples to 216 and 204 kOe for cobalt-free samples, respectively. The hyperfine field $H_{eff}(T)$ reduces by ~7 kOe per at % chromium.

3.2. Mössbauer studies of a-$Fe_{74}Co_5Cr_5B_{16}$

As a representative study of the entire family of the amorphous alloys containing chromium, a-$Fe_{74}Co_{10-x}Cr_xB_{16}$ (x = 0, 2.5, 5, 7.5 and 10) alloys, the hyperfine interactions for the middle member of the family, a-$Fe_{74}Co_5Cr_5B_{16}$, is extensively studied as a function of temperature (5 to 800 K). The spectra of the samples recorded at different temperatures are shown in Fig. 3.

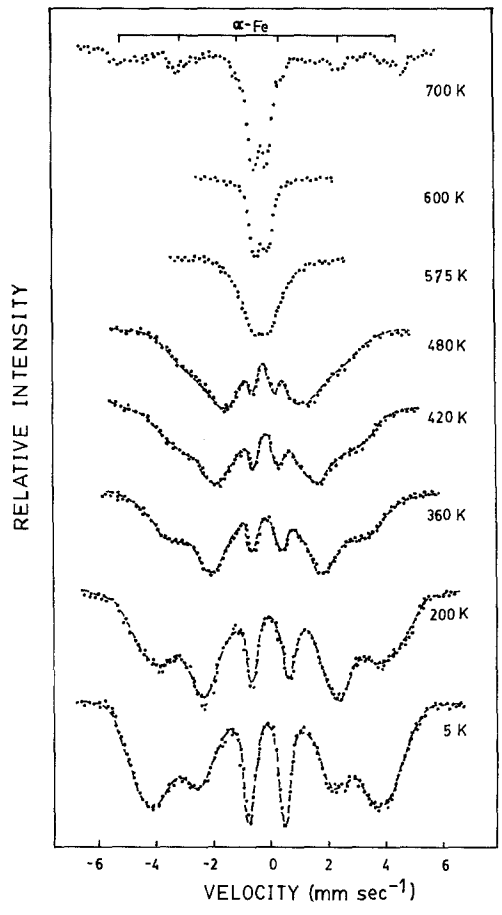

Figure 3 Mössbauer spectra of a-$Fe_{74}Co_5Cr_5B_{16}$ at different temperatures. Dashed line, theoretical spectra according to Window [24].

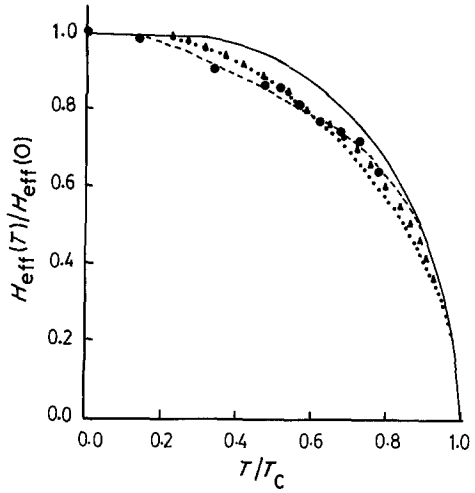

Figure 4 Plot of reduced average hyperfine field against reduced temperature for a-$Fe_{74}Co_5Cr_5B_{16}$. (——) Brillouin curve for $S = 1$; (· · ·) Handrich's curve for $\delta = 0.4$ and $S = 1$; (— —) curve of Prasad *et al.* for $\delta = 0.6$ and $S = 1$; ▲ Kaneyoshi and Tamura's curve for $\delta_0 = 0.33$, $S = 1$, $\alpha = 0.5$, $n = 1.25$ and $Z^* = 12$; (●) experimental data.

The spectra up to 480 K exhibit six-line patterns characterized by broad asymmetrical lines, with variation in their line widths from 0.4 to 2.02 mm sec^{-1}. For instance, the line widths of the spectrum recorded at 298 K for the present case are 2.02 : 1.34 : 0.41 : 0.88 : 1.17 : 1.88 mm sec^{-1} for the first to sixth lines, respectively. The average line widths for the pairs increase from the inner pair (3, 4) to the outer pair (1, 6). The spectra recorded above 480 K and below 575 K exhibit broad unresolved profiles, with overlapping lines indicating the presence of hyperfine interactions. However, at 575 K the sample exhibits an asymmetric quadrupole doublet with an average splitting of 0.42 ± 0.03 mm sec^{-1}. The doublet spectra recorded at 600, 640 and 670 K also exhibit pronounced asymmetry in their profiles. At 700 K, the spectrum is characterized by additional peaks along with the paramagnetic doublet (Fig. 3). The additional lines were found to correspond to the hyperfine field split Mössbauer spectrum of α-iron. In other words, the sample exhibits the onset of crystallization (T_x) at 700 K with precipitation of α-iron.

The magnetic hyperfine field $H_{eff}(T)$, obtained from the least-square fit of the spectra below T_c, shows a decreasing trend with increase in temperature. The saturation magnetic hyperfine field, $H_{eff}(0)$, obtained from the plot $H_{eff}(T)$ against temperature on extrapolation to $T = 0$ K, is found to be 276 ± 3 kOe. Fig. 4 shows the plot of reduced average hyperfine field, $H_{eff}(T)/H_{eff}(0)$ against reduced temperature, T/T_c for this sample along with the theoretical Brillouin curve for spin $S = 1$. The reduced field data deviate from the Brillouin curve. According to Handrich, the deviation can be accounted for using the expression of the form [28],

$$\sigma = \frac{H_{eff}(T)}{H_{eff}(0)} = \tfrac{1}{2}B_s[(1 + \delta)x] + \tfrac{1}{2}B_s[(1 - \delta)x] \quad (2)$$

where $x = [3S/(S + 1)](\sigma/t)$, $t = T/T_c$ and $\delta^2 = \Delta J^2/< J^2 > \cdot \delta$ is the measure of fluctuations in exchange integral, J, the value of which lies between 0 and 1. B_s is the Brillouin function for spin S. The theoretical curve generated with δ and S as variables, which showed close agreement with the experimental data, is also shown in Fig. 4. The agreement with experimental data can be considerably improved by assuming a temperature dependent δ of the form $\delta(T) = \delta_0(1 - t^2)$ [15, 17, 29]. The theoretical curve thus generated shows better agreement with the experimental data (Fig. 4). Fig. 4 also shows the theoretical curve according to Kaneyoshi and Tamura [30] assuming $\delta(T)$ in Handrich's relationship to be

$$\delta(T) = \sqrt{\delta_0^2 + \left(\delta_0^2 + \frac{1}{Z^*}\right) 1(T, 0)} \quad (3)$$

where $1(T, 0) = \alpha[1 - t^n]$, and Z^* is the effective coordination number.

TABLE II The most probable field (H_p), mean field (H_{mean}) and full width at half maximum (ΔH) for a-$Fe_{74}Co_5Cr_5B_{16}$ alloys at different temperatures according to Window [24].

Temperature (K)	H_p (± 3 kOe)	H_{mean} (± 3 kOe)	ΔH (± 3 kOe)
5	276.8	253.5	123.8
200	261.0	244.9	128.3
273	238.5	226.1	166.5
330	225.6	216.5	180.0
390	211.5	202.5	166.0
420	193.5	197.0	150.8

The hyperfine field distribution curves obtained for the spectra at 5, 200, 320, 390, 420 and 450 K by the method of Window [24] are reproduced in Fig. 5. The H_p and H_{mean} values determined from the $P(H)$ curves are listed in Table II. The individual line widths of the quadrupole split spectra at 600, 640 and 670 K were large (0.45 mm sec^{-1}), indicating a distribution in electric field gradients, $P(QS)$. The $P(QS)$ distribution has been extracted from the experimental doublet spectra according to Le Cäer and Dubois [27, 31]. In this method a linear correlation between isomer shift and quadrupole splitting of the form

$$IS = a(QS - QS_0) + b \quad (4)$$

where a and b are the correlation parameters, and QS_0 is the lower limit of QS, (in our case 0.1 mm sec^{-1}) is found to give good agreement with the experimental spectra (Fig. 6). In the above fit, a and b were treated as variables to get the best fit. The peak quadrupole splitting, QS_p, the mean quadrupole splitting, QS_{mean}, the full width at half maximum of the $P(QS)$ distribution, ΔQS and a and b values are listed in Table III. The average isomer shifts, IS, calculated from $P(QS)$ distribution curves is in the range 0.30 to 0.38 mm sec^{-1} (Fe).

The average hyperfine field data, as obtained from the least-square fit of Mössbauer spectra measured at different temperatures, can be used for the verification of the applicability of spin wave theory in amorphous solids using the relationship [17, 32],

$$\frac{H_{eff}(T) - H_{eff}(0)}{H_{eff}(0)} = -BT^{3/2} - CT^{5/2}$$

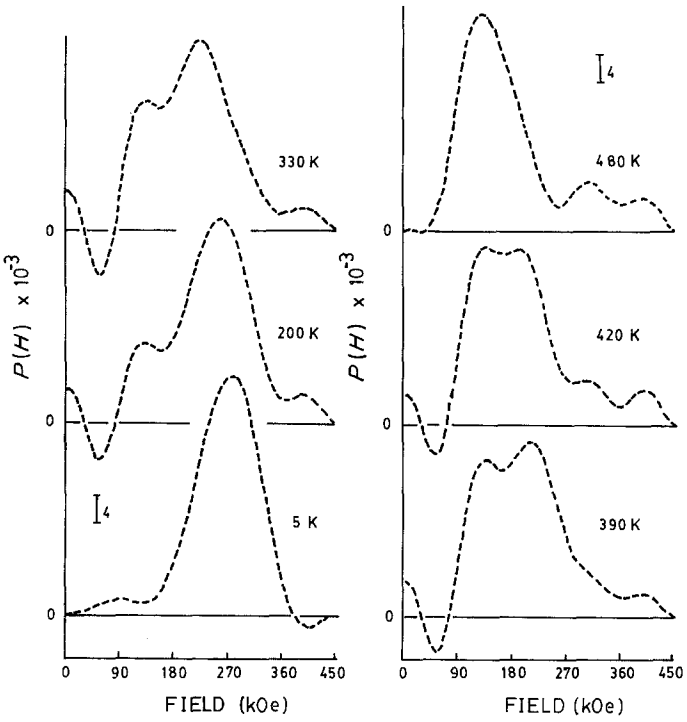

Figure 5 $P(H)$ curves obtained for a-$Fe_{74}Co_5Cr_5B_{16}$ at different temperatures according to Window [24].

or

$$\frac{H_{\text{eff}}(T) - H_{\text{eff}}(0)}{H_{\text{eff}}(0)} = -B_{3/2}(T/T_c)^{3/2} - C_{5/2}(T/T_c)^{5/2} \quad (5)$$

where $B_{3/2}$, $C_{5/2}$, B and C are spin-wave coefficients. For the extraction of the values for these coefficients, $[H_{\text{eff}}(T) - H_{\text{eff}}(0)]/H_{\text{eff}}(0)$ plotted against $(T/T_c)^{3/2}$ is shown in Fig. 7. From this figure it is seen that the experimental data do follow a linear behaviour up to $T/T_c = 0.60$. The slope of the plot gives a value of $B_{3/2} = 0.43 \pm 0.03$. A least-square fit of the above equation in the temperature range $0.0 < T/T_c > 0.60$ gave rise to the values $B_{3/2} = 0.50$, $C_{5/2} = 0.17$, $B = 36.3 \times 10^{-6}\,K^{-3/2}$ and $C = 2.17 \times 10^{-8}\,K^{-5/2}$. The hyperfine field data of a-$Fe_{74}CO_5Cr_5B_{16}$ may be used to evaluate the critical exponents β and D from the power law of the form [17, 29],

$$\frac{H_{\text{eff}}(T)}{H_{\text{eff}}(0)} = D[1 - T/T_c]^{\beta} \quad (6)$$

The plot of $H_{\text{eff}}(T)/H_{\text{eff}}(0)$ against $(1 - T/T_c)$ on a log–log scale is shown in Fig. 8. The slope of the linear plot yielded β value of 0.41 ± 0.03. The least-square fit of the experimental data to Equation 6 in the temperature range $0.78 < T/T_c < 0.6$ led to values for β and D of 0.47 ± 0.03 and 1.19 ± 0.03, respectively.

4. Discussion

The Mössbauer spectra of the a-$Fe_{74}Co_{10-x}Cr_xB_{16}$ (x = 0, 2.5, 5, 7.5 and 10) alloys at 80 K exhibit asymmetry with broad resonance lines. The line widths are comparatively higher than that of natural iron (0.19 mm sec^{-1}). The broadening of the spectral lines arise due to the random distribution on non-equivalent iron sites. The relative intensities observed for the spectra as a function of chemical composition and temperature are characteristic features of iron-rich amorphous alloys [17–21]. In the case of spectra recorded at 80 K, the ratio $A_{2,5}/A_{1,6}$ shows a significant change. This corresponds to a variation of Θ from 44° for $x = 0$ to 18° for $x = 10$ samples. Thus, it is clear that the introduction of an increasing amount of chromium brings about a significant change in the orientation of the magnetization axis, bringing it closer to the direction of γ-ray propagation. The spectra of a-$Fe_{74}Co_5Cr_5B_{16}$ recorded in the temperature range 5 to 480 K (Fig. 2) also shows a perceptible change in the ratio of $A_{2,5}/A_{1,6}$, indicating that the orientation of the magnetization axis also changes as a function of temperature. The Curie temperature of these samples falls systematically with increasing chromium content at a rate of 30 K per at % chromium. Recently, Akhtar *et al.* have reported their differential scanning calorimetric studies on the thermal behaviour of these samples [12]. They show that the onset of crystallization takes place at higher temperatures with increasing chromium content, ranging from 688 K for $x = 0$ samples to 763 K for $x = 10$ samples. Thus, while thermal stability improves as shown by a rise in T_x of

TABLE III Peak quadrupole splitting (QS_p), mean quadrupole splitting (QS_{mean}), FWHM of $P(QS)$ distribution (ΔQS) and a and b parameters according to Le Cäer and Dubois [27].

Temperature (K)	QS_p (± 0.02 mm sec^{-1})	QS_{mean} (± 0.02 mm sec^{-1})	ΔQS (± 0.02 mm sec^{-1})	a	b
600	0.43	0.43	0.09	−0.13	−0.23
640	0.45	0.44	0.09	−0.20	−0.22
670	0.43	0.44	0.09	−0.22	−0.25

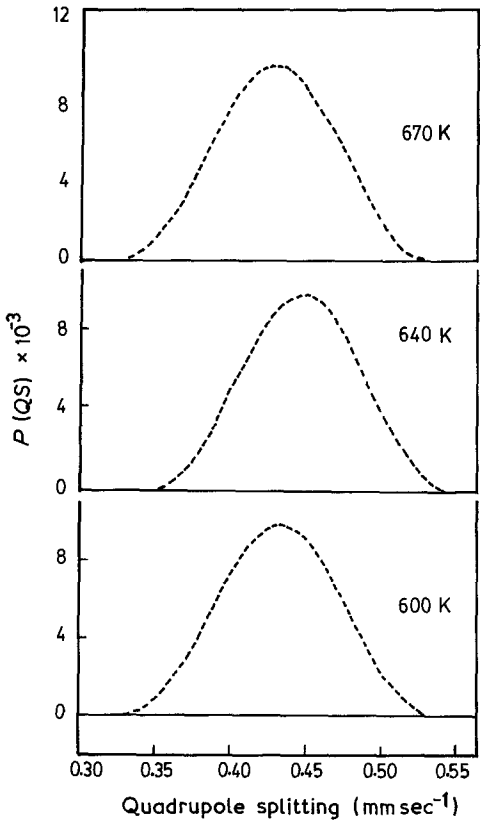

Figure 6 $P(QS)$ distribution curves of a-$Fe_{74}Co_5Cr_5B_{16}$ at different temperatures according to Le Cäer and Dubois [27].

10 K per at % chromium, it brings about a significant fall in the Curie temperature.

The H_p and H_{mean} values obtained from $P(H)$ curves for the spectra recorded at 80 K show a systematic fall with increasing chromium content. This trend parallels with the fall in Curie temperature. On the other hand, the ΔH values show a systematic increase. This arises due to the increasing contribution to the hyperfine field in the lower region caused by increasing Fe–Cr antiferromagnetic exchange interactions [18, 21, 34, 35]. This is also evident from the increasing asymmetry in the $P(H)$ profiles of the major peak with increasing chromium content. For a given sample of a-$Fe_{74}Co_5Cr_5B_{16}$, the H_p and H_{mean} values show a systematic fall with increasing temperature. This is to be expected, as the hyperfine field decreases with increasing temperature [36–38]. The change in the $P(H)$ profiles and increase in ΔH values with increasing temperature arise due to increasing contributions to the hyperfine field in the low-field

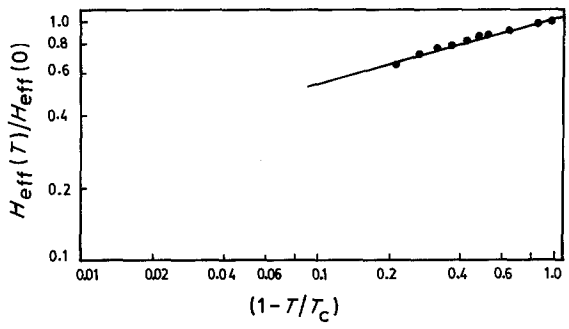

Figure 7 Plot of fractional hyperfine field against $(T/T_c)^{3/2}$ for a-$Fe_{74}Co_5Cr_5B_{16}$. $\Delta H = H_{eff}(T) - H_{eff}(0)$.

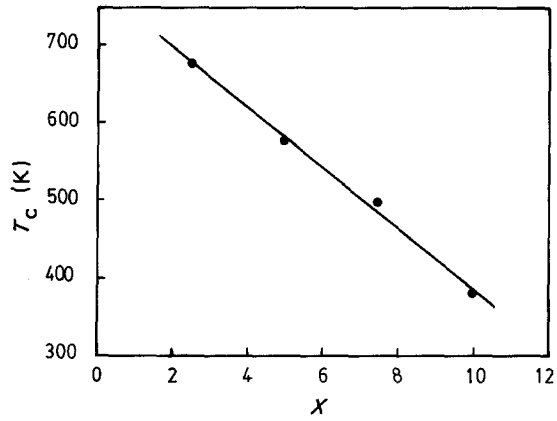

Figure 8 Plot of $H_{eff}(T)/H_{eff}(0)$ against $(1 - T/T_c)$ for a-$Fe_{74}Co_5Cr_5B_{16}$ on log-log scale.

region, with the major peak shifting to lower field values and the contributions to the lower range of the hyperfine fields remaining unaffected by temperature. The observed variations in the ΔH values as a function of temperature also indicate that different hyperfine fields exhibit different temperature dependences [21]. The observed asymmetry and the large ΔH values, > 123 kOe compared to 90 kOe in ternary amorphous alloys, show the presence of a bimodal distribution of hyperfine fields [21, 39, 40]. In the present alloys, too, the bimodal distribution arises due to two types of randomly packed cells, one rich in chromium and the other in iron, the former making a significant contribution at low fields. Such bimodality has been observed in other amorphous alloys containing chromium and molybdenum [9, 19–21].

The deviation of experimental data from the theoretical Brillouin curve is the characteristic feature of iron-rich amorphous alloys [17, 23, 41–44]. Handrich's formulation qualitatively accounts for such a deviation, assuming a fluctuation in the exchange interactions. However, when δ is assumed to be temperature dependent the agreement is closer, although the expression of Prasad *et al.* is empirical in nature. The model of Kaneyoshi and Tamura [30] no doubt rationalizes the temperature dependence of δ through the temperature dependence of the distribution of magnetic moments, but their final expression shows less agreement with the experimental data than the empirical fit of Prasad *et al* [15–17, 29].

The $P(QS)$ distribution in amorphous alloys is interesting, and such analyses have been reported for a-$Fe_{15}Ni_{60}Si_{10}B_{15}$ [31], a-$Fe_{35}Ni_{40}Si_{10}B_{15}$ [45], a-$Fe_{1-x}Mo_x$ and a-$Fe_{1-x}Ti_x$ alloys [46, 47]. Our results are in close agreement with those reported earlier. The chief distinction between amorphous alloys, including those under present study and the crystalline systems, is found to be that the electric field gradients in amorphous alloys do not show any temperature dependence. It may therefore be concluded that the observed quadrupole splitting is caused by contributions to the electric field gradient by charge transfer between metal–metalloid bonds. The charge-transfer mechanism in amorphous alloys has been suggested by Mizoguchi *et al.* to explain magnetic moment variations [48]. In such a case, one would expect no

significant change in the electronic population in the energy levels available, leading to a temperature-independent electric field gradient.

In contrast to crystalline ferromagnets such as iron and nickel, a-$Fe_{74}Co_5Cr_5B_{16}$ exhibits a linear relationship of $T^{3/2}$ dependence over a wide temperature range (Fig. 7); this seems to be a common property of many amorphous alloys [17, 49–52]. Simpson [53] has shown that the high values for the coefficients B and C observed in these alloys arise due to the high disorder characteristic of the amorphous solids. Furthermore, the larger values for B and C show that the random distribution of atoms in amorphous matrix favours the excitation of long-wavelength spin waves with relative ease over a large temperature interval. The critical exponent β and D determined from the power law are typical of metallic glasses [54–58]. Many of the amorphous solids studied do exhibit β values close to ~ 0.40, which is definitely greater than the theoretical value of $\beta = 0.3647 \pm 0.0002$ for 3-d Heisenberg ferromagnets [59]. It has been suggested on the basis of theoretical calculations that missing exchange bonds and the presence of defects can lead to an enhancement in the β value [60]. Alternatively, alloys of the present type, in which chromium is present, can give rise to magnetic inhomogeneity leading to an apparently large β value. In such cases, careful analysis resolving the data on the basis of two environments present due to magnetic inhomogeneity can lead to a close match with the theoretically predicted values for 3-d Heisenberg ferromagnets, as shown in susceptibility studies of such alloys [54–57].

5. Conclusions

A new family of a-$Fe_{74}Co_{10-x}Cr_xB_{16}$ ($x = 0, 2.5, 5, 7.5$ and 10) alloys has been prepared for the first time to study the influence of chromium on magnetic properties and the thermal stability of these alloys. It is established that chromium can replace cobalt entirely in a-$Fe_{74}Co_{10-x}Cr_xB_{16}$, giving rise to a-$Fe_{74}Cr_{10}B_{16}$. The effective hyperfine field, $H_{\text{eff}}(T)$, determined for the spectra recorded at 80 K and the Curie temperature of these samples, show a systematic decrease with increasing chromium content on account of antiferromagnetic exchange interactions between iron and chromium. The analysis of relative line intensities of Mössbauer spectra at 80 K show that the magnetization axis tends to come closer to the direction of γ-ray propagation with increasing chromium content. The hyperfine field distribution shows increasing asymmetry and higher ΔH values with increasing chromium content, caused by the increasing contribution to the lower values of hyperfine fields on account of antiferromagnetic exchange interactions.

The middle member of the family a-$Fe_{74}Co_5Cr_5B_{16}$, which is studied in detail as a representative member (5 to 800 K), shows anomalous temperature dependence of hyperfine fields, typical of iron-rich amorphous alloys. The flattening in the reduced field against reduced temperature curve, resulting in deviation from the theoretical Brillouin curve, can be accounted for on the basis of Handrich's formulation, the theoretical model of Kaneyoshi and Tamura [30], or using the empirical relationship of Prasad *et al.* The closest agreement, however, is shown by the expression of Prasad *et al.* The features of field distribution curves can be explained on the basis of different hyperfine fields exhibiting different temperature dependences and two types of randomly packed cells, one rich in chromium and the other in iron, giving rise to bimodality in the field distribution. The distribution in quadrupole splitting determined from the paramagnetic doublet spectra is found to be temperature independent, showing that the electric field gradient arises due to a charge transfer mechanism. The temperature dependence of hyperfine fields at low temperatures gives evidence for long-wavelength spin-wave excitations. Using the hyperfine field data close to T_c, critical exponent β and D values were determined from the power law to be 0.47 ± 0.03 and 1.19 ± 0.03, respectively. The deviation of the value of β from that of the theoretical value for 3-d Heisenberg ferromagnets is attributed to magnetic inhomogeneity.

Acknowledgements

It is a pleasure to thank Professor P. Rama Rao for his encouragement and permission to publish this work. One of us (T.G.N.) thanks the Council of Scientific and Industrial Research, New Delhi, for a doctoral fellowship.

References

1. F. E. LUBORSKY, (ed.), "Amorphous Metallic Alloys" (Butterworth, Boston, 1983).
2. K. MOORJANI and J. M. D. COEY, "Magnetic Glasses" (Elsevier, Amsterdam, 1984).
3. M. R. J. GIBBS and H. G. HYGATE, *J. Phys. F* **16** (1986) 809.
4. R. A. DUNLAP, J. E. BALL and K. DINI, *J. Mater. Sci. Lett.* **4** (1985) 773.
5. R. B. DIEGLE, *J. Non-Cryst. Solids* **61-62** (1984) 601.
6. I. W. DONALD, T. KEMENY and H. A. DAVIES, *J. Phys. F* **11** (1981) L131.
7. H. J. V. NIELSEN, *J. Magn. Magn. Mater.* **12** (1979) 187.
8. *Idem, Solid State Commun.* **30** (1979) 239.
9. C. L. CHIEN and H. S. CHEN, *J. Appl. Phys.* **50** (1979) 1574.
10. S. DEY, *et al., J. Appl. Phys.* **52** (1981) 1805.
11. D. AKHTAR and V. CHANDRASEKARAN, *J. Mater. Sci. Lett.* **4** (1985) 1465.
12. D. AKHTAR, V. N. MURTHY, P. SUBRAHMANIAM and R. JAGANNATHAN *ibid.* **5** (1986) 1148.
13. V. N. MURTHY, D. AKTAR, R. SUBRAHMANIAM, R. JAGANNATHAN and T. G. N. BABU, *Mater. Res. Bull.* **21** (1986) 1299.
14. R. P. MATHUR, V. N. MURTHY, D. AKHTAR, P. SUBRAHMANIAM and R. JAGANNATHAN, *J. Mater. Sci. Lett.* **6** (1987) 1019.
15. B. B. PRASAD, A. K. BHATNAGAR and R. JAGANNATHAN, *J. Appl. Phys.* **54** (1983) 2019.
16. *Idem, Solid State Commun.* **36** (1980) 661.
17. A. K. BHATNAGAR, B. B. PRASAD and R. JAGANNATHAN, *Phys. Rev. B* **29** (1984) 4896.
18. V. SRINIVAS, G. RAJARAM, S. PRASAD, G. CHANDRA, S. N. SHRING, R. KRISHNAN and P. ROUGIER, *Hyp. Inter.* **34** (1987) 495.
19. R. A. DUNLAP and G. STROINK, *Can. J. Phys.* **62** (1984) 714.
20. *Idem, J. Phys. F* **14** (1984) 3083.
21. C. L. CHIEN, *Phys. Rev. B* **19** (1979) 81.
22. P. J. SCHURER and A. H. MORRISH, *J. Magn. Mag. Mater.* **15-18** (1980) 577.

23. C. L. CHIEN, D. MUSSER, E. M. GYORGY, R. C. SHERWOOD, H. S. CHEN, F. E. LUBORSKY and J. L. WALTER, *Phys. Rev. B* **20** (1979) 283.
24. B. WINDOW, *J. Phys. E* **4** (1971) 401.
25. J. HESSE and A. RUBARTSCH, *ibid.* **7** (1974) 526.
26. P. MANGIN, G. MARCHAL, M. PIECUCH and C. JANOT, *ibid.* **9** (1976) 1101.
27. G. LE CAER and J. M. DUBOIS, *ibid.* **12** (1979) 1032.
28. K. HANDRICH, *Phys. Stat. Solidi* **32** (1969) K55.
29. A. K. BHATNAGAR, B. B. PRASAD, N. RAVI, R. JAGANNATHAN and T. R. ANANTHARAMAN, *Solid State Commun.* **44** (1982) 905.
30. T. KANEYOSHI and I. TAMURA, *Phys. Stat. Solidi* (*b*) **123** (1984) 525.
31. M. KOPCEWICZ, B. KOPCEWICZ and U.GONSER, *J. Magn. Magn. Mater.* **66** (1987) 79.
32. F. BLOCH, *Z. Phys.* **61** (1930) 206.
33. *Idem, ibid.* **74** (1932) 295.
34. W. S. CHAN, B. G. SHEN, H. Y. LO and B. L. YU, in Proceedings of the 4th International Conference on Rapidly Quenched Metals Vol. II, edited by T. Masumoto and K. Suzuki (Sendai, 1981) p. 1137.
35. A. T. ALDRED, B. D. RAINFORD, J. S. KOUVEL and J. J. HICKS, *Phys. Rev. B* **14** (1976) 228.
36. W. MARSHALL, *Phys. Rev.* **110** (1958) 1280.
37. R. S. PRESTON, S. S. HANNA and J. HEBERLE, *Phys. Rev. B* **128** (1962) 2207.
38. J. G. DASH, B. D. DUNLAP and D. G. HOWARD, *Phys. Rev.* **141** (1966) 376.
39. G. L. WHITTLE, S. J. CAMPBELL and A. M. STEWART, *Phys. Stat. Solidi* (*a*) **70** (1982) 245.
40. I. M. TANG, *J. Magn. Magn. Mater.* **53** (1985) 233.
41. I. VINCZE, F. VAN DER WOUDE, T. KEMENEY and A. S. SHAAFSMA, *J. Magn. Magn. Mater.* **15-18** (1980) 1336.
42. S. N. KAUL, *Phys. Rev. B* **24** (1981) 6550.
43. F. E. LUBORSKY, J. L. WALTER, H. H. LIEBERMANN and E. P. WOHLFARTH, *ibid.* **15-18** (1980) 1351.
44. H. YAMAMOTO, H. ONODERA, K. HOSOYAMA, T. MASUMOTO and Y. YAMAUCHI, *ibid.* **31-34** (1983) 1579.
45. M. KOPCEWICZ, H. G. WAGNER and U. GONSER, *J. Phys. F* **16** (1986) 929.
46. K. SUMIYAMA, H. EZAWA and Y. NAKAMURA, *J. Phys. Chem. Solids* **48** (1987) 255.
47. *Idem, Phys. Stat. Solidi* (*a*) **93** (1986) 81.
48. T. MIZOGUCHI, K. YAMAUCHI and H. MIYAJIMA, in "Amorphous Magnetism", edited by H. O. Hooper and A. M. De Graaf (Plenum, New York, 1973) p. 325.
49. R. C. COCHRANE and C. S. CARGIL III, *Phys. Rev. Lett.* **32** (1974) 476.
50. S. N. KAUL, *Phys. Rev. B* **27** (1983) 5761.
51. M. EIBSCHUTZ and M. E. LINES, *ibid.* **7** (1973) 4907.
52. B. E. ARGYLE, S. H. CHARAP and E. W. PUGH, *Phys. Rev.* **132** (1963) 2051.
53. A. W. SIMPSON, *Wiss. Z. Tech. Univ. Dres.* **3** (1974) 1020.
54. S. N. KAUL, *IEEE Trans. Magn.* **MAG-20** (1984) 1290.
55. *Idem, Phys. Rev. B* **22** (1988) 278.
56. S. N. KAUL and M. ROSENBERG, *Solid State Commun.* **41** (1982) 857.
57. T. KANEYOSHI, *J. Phys. Soc. Jpn.* **51** (1982) 73.
58. K. BINDER and P. C. HOHENDERG, *Phys. Rev. B* **9** (1974) 2194.
59. J. C. LEGUILLOU and J. ZINN-JUSTIN, *Phys. Rev. Lett.* **39** (1975) 95.
60. S. J. POON and J. DURAND, *Phys. Rev. B* **16** (1977) 316.

Received 1 March
and accepted 30 August 1989